International Journal of Medical Sciences
ISSN 1449-1907 www.medsci.org 2008 5(5):273-284

Research Paper

TMZ-BioShuttle – a reformulated Temozolomide

Waldemar Waldeck[1], Manfred Wiessler[2], Volker Ehemann[3], Ruediger Pipkorn[4], Herbert Spring[5], Juergen Debus[6], Bernd Didinger[6], Gabriele Mueller[1], Joerg Langowski[1], Klaus Braun[2] ✉

1. German Cancer Research Center, Division of Biophysics of Macromolecules, INF 580, D-69120 Heidelberg, Germany
2. German Cancer Research Center, Dept. of Molecular Toxicology, INF 280, D-69120 Heidelberg, Germany
3. University of Heidelberg, Institute of Pathology, INF 220, D-69120 Heidelberg, Germany
4. German Cancer Research Center, Central Peptide Synthesis Unit, INF 580, D-69120 Heidelberg, Germany
5. German Cancer Research Center, Dept. of Structural Analysis of Gene Structure and Function, INF 280, D-69120 Heidelberg, Germany
6. University of Heidelberg, Dept. of Radiation Oncology, INF 400, D-69120 Heidelberg, Germany

✉ Correspondence to: Dr. Klaus Braun, German Cancer Research Center (DKFZ), Dept. Molecular Toxicology, Im Neuenheimer Feld 280, D-69120 Heidelberg, Germany. Phone: +49 6221-42 2495; Fax: +49 6221-42 3375; e-mail: k.braun@dkfz.de

Received: 2008.08.18; Accepted: 2008.09.12; Published: 2008.09.15

There is a large number of effective cytotoxic drugs whose side effect profile, efficacy, and long-term use in man are well understood and documented over decades of use in clinical routine e.g. in the treatment of recurrent glioblastoma multiforme (GBM) and the hormone-refractory prostate cancer (HRPC). Both cancers are insensitive against most chemotherapeutic interventions; they have low response rates and poor prognoses. Some cytotoxic agents can be significantly improved by using modern technology of drug delivery or formulation. We succeeded to enhance the pharmacologic potency with simultaneous reduction of unwanted adverse reactions of the highly efficient chemotherapeutic temozolomide (TMZ) as an example. The TMZ connection to transporter molecules (TMZ-BioShuttle) resulted in a much higher pharmacological effect in glioma cell lines while using reduced doses. This permits the conclusion that a suitable chemistry could realize the ligation of pharmacologically active, but sensitive and highly unstable pharmaceutical ingredients without functional deprivation. The re-formulation of TMZ to TMZ-BioShuttle achieved a nearly 10-fold potential of the established pharmaceutic TMZ far beyond the treatment of brain tumors cells and results in an attractive reformulated drug with enhanced therapeutic index.

Key words: BioShuttle, Carrier Molecules; Drug Delivery; facilitated Transport; Glioblastoma multiforme (GBM); Reformulation, Temozolomide (TMZ)

Introduction

The medicinal treasures in the pharmacopoeia worldwide, harboring multi-faced monographs, whose pharmacologic potential albeit their therapeutic limits are well known. New formulations of conventional cytotoxic drugs may open a door to a new quality of the pharmaceutical research. This redesign of "old fashioned" molecules to highly active pharmaceutical ingredients (API) could be a suitable practice capable of improve the therapeutic index [1-4]. In case of malignant brain tumors especially in the chemotherapy of glioblastoma multiforme (GBM) the anti cancer drug temozolomide (TMZ) (8-carbamoyl-3-methylimidazo [5,1-d]-1,2,3,5-tetrazin-4(3*H*)-one) has been well studied [5, 6]. It has been shown in recent phase III study, that a simultaneous therapy with TMZ improves survival rates for patients with GBM treated with radiotherapy [7]. Encouraging data [8] give reason to expand the intervention with TMZ to difficult tumor types like prostate cancer. Under clinical conditions TMZ was absorbed rapidly into the blood, and spontaneously decomposed at physiological pH to the cytotoxic methylating agent 5-(3-methyltriazeno)-imidazole-4-carboxamide (MTIC). Its half-life and apparent oral systemic clearance values were 1.8 hours and 97 ml/minute/m^2, however neutropenia and thrombocytopenia limited the tolerable application doses to 1000 mg/m^2. The cytotoxicity of TMZ appears to be elicited through adduction of methyl groups to O^6 positions of guanine (O^{6}mG) in genomic DNA [9] followed by recognition of this adduct by the mismatch repair system (MMR), which can mispair with thymine during the next cycle of DNA replication [10, 11].

The half-life of TMZ [12] in plasma and the non-target-gene-specific alkylating mode of action can lead to undesired adverse reactions, which could result in discontinuation or interruption of therapy. TMZ therefore seems to be a good candidate for reformulation, since our new TMZ derivatives could circumvent these problems by retaining the high efficiency but not the adverse effects of TMZ.

The coupling of a peptide-based nuclear localization sequence (NLS) leads to an active nuclear targeting minimizing the above described handicaps (Drug Design, Development and Therapy, in press). But due to their higher molecular mass and their physico-chemical characteristics the transport of TMZ-NLS peptide conjugates alone across the cellular membrane is poor. Therefore a transport molecule is needed so that a sufficient concentration of pharmacologically active molecules can reach their target side inside the nucleus.

Our efforts resulted in suitable ligation modes of TMZ with a nuclear address peptide which in turn is connected to carrier molecules. For a better understanding a definition for "ligation" is given in chemistry the meaning of "ligation reaction" is the basis of the Diels-Alder chemistry, which we focus on here.

Such a ligation reaction should meet the following criteria: (1) rapid course of the reaction, (2) independent from solvent properties, (3) no side reaction with other functional groups present in the molecules, (4) without additional coupling-reagents, (5) irreversible chemical reaction characteristics, and (6) an economical procedure.

Our concept is based on the 'Click Chemistry'. It's applications are increasingly found in all aspects of drug discovery, ranging from clue finding through combinatorial chemistry and target-templated *in situ* chemistry, to proteomics and DNA research, using Staudinger and Sharpless conjugation reactions [13-16]. In this regard the 1,3-dipolar cycloaddition developed by Huisgen has to be considered as a 'cream of the crop' [17].

Our ligation approach is based on cycloaddition reactions via the pericyclic Diels Alder Reaction (DAR) with 'inverse-electron-demand' (DAR_{inv}), which is a modification of π-electron-deficient N-heteroaromatics with electron-rich dienophils [18]. The DAR_{inv} is, in contrast to DAR, irreversible with the compounds we used. In this way the pharmaceutic TMZ was coupled to the modularly structured carrier. We called it TMZ-BioShuttle. During biological tests we reached a dramatically increased efficiency in two different tumor cell lines in the glioblastoma cell line TP 366 and in the human prostate cancer cell line DU 145.

The analyses of dilution series indicated for the application of the TMZ-BioShuttle that the spectra of the treatable tumor types could be extended.

Materials and Methods

Synthesis of the TMZ-derivative

A 0.2 mol preparation with 42.7 mg 4-methyl-5-oxo-2,3,4,6,8-pentazabicyclo[4.3.0]nona-2,7,9-trien-9-carboxylic acid chloride and 67.4 mg modified tetrazine as well as 28 µl triethylamine were dissolved in chloroform. The reaction process runs undisturbed and provides a defined product with the molecular weight (MW) m/e 513.

Synthesis of the Boc-Lys(TCT)-OH

42 mg cyclooctotetraen and 44 mg maleic acid anhydride were resolved in chloroform and methanol 1 %. The chemical reaction is described by Reppe [19].

Solid phase peptide synthesis of the BioShuttle transporter

For solid phase synthesis of the K(TCT)-NLS-S∩S-transmembrane transport peptide the Fmoc-strategy was employed in a fully automated multiple synthesizer (Syro II) [20]. The synthesis was carried out on a 0.05mmol Fmoc-Lys(Boc)-polystyrene resin 1% crosslinked and on a 0.053 mmol Fmoc-Cys(Trt)-polystyrene resin (1% crosslinked). As coupling agent 2-(1H-Benzotriazole-1-yl)-1,1,3,3-tetramethyluronium hexafluorophosphate (HBTU) was used. The last amino acid of the NLS-peptide was incorporated as Boc-Lys(TCT)-OH. Cleavage and deprotection of the peptide resin were affected by treatment with 90% trifluoroacetic acid, 5% ethanedithiol, 2.5% thioanisole, 2.5% phenol (v/v/v/v) for 2.5 h at room temperature. The products were precipitated in ether. The crude material was purified by preparative HPLC on an Kromasil 300-5C18 reverse phase column (20 × 150 mm) using an eluent of 0.1% trifluoroacetic acid in water (A) and 60% acetonitrile in water (B). The peptides were eluted with a successive linear gradient of 25% B to 60% B in 40 min at a flow rate of 20 ml/min. The fractions corresponding to the purified protein were lyophilized.

Coupling of the transmembrane carrier - and the K(TCT)-NLS-Cys-module

The K(TCT)-NLS-C and the transport peptide were oxidized in an aqueous solution of 2mg/ml in 20% DMSO. After five hours the reaction was complete. The oxidation progress was monitored by analytical C18 reversed-phase HPLC, and then the peptide was purified as described above. The purified material

was characterized with analytical HPLC and laser desorption mass spectrometry in a Bruker Reflex II.

Reagents and cell culture

Human glioblastoma (GBM) primary cells (TP 366) [21] and human prostate cancer cells (DU 145) [22] were provided by the DKFZ division of Biophysics of Macromolecules. All cell lines were cultured in DMEM (Gibco Cat. No. 12800) supplemented with 10% FCS and maintained in culture at 37°C with 5% CO_2 atmosphere and 95% humidity.

Chemotherapy treatment

Pure temozolomide (TMZ) was purchased from Sigma-Aldrich, Germany (Cat. No. 76899) and the material was subdivided into two parts for subsequent processing. One part was followed up and coupled to the transporter molecules. As a control, the second part was dissolved in acetonitrile 10% (Sigma-Aldrich, Germany) with a final concentration of 0.2% acetonitrile.

DU 145 and TP 366 cells were seeded (1×10^5 cells/ml) in DMEM (control) and in DMEM containing a dilution series of TMZ and of TMZ-BioShuttle from 50 to 6.25 µM respectively. The behavior of the cells was up to 6 days.

Cell Cycle Analysis

The effects on the cell cycle distribution were determined by DNA flow cytometry. Flow cytometric analyses were performed using a PAS II flow cytometer (Partec, Muenster, Germany) equipped with a mercury vapor lamp (100 W) and a filter combination for 2,4-diamidino-2-phenylindole (DAPI) stained single cells. From native probes the cells were isolated with 2.1% citric acid/ 0.5% Tween 20 according to the method for high resolution DNA and cell cycle analyses [23] at room temperature. Phosphate buffer (7.2g $Na_2HPO_4 \times 2H_2O$ in 100ml H_2O dest.) pH 8.0 containing DAPI for staining the cell suspension was performed. Each histogram represents 30.000 cells for measuring DNA-index and cell cycle. For histogram analysis, we used the Multicycle program (Phoenix Flow Systems, San Diego, CA).

Cell viability

For detection of apoptotic cells and viability, a FACS Calibur flow cytometer (Becton Dickinson Cytometry Systems, San Jose, CA) was used with filter combinations for propidium iodide. For analyses and calculations, the Cellquest program (Becton Dickinson Cytometry Systems, San Jose, CA) was carried out. Each histogram and dot plot represents 10.000 cells. After preparation according to Nicoletti [24] with modifications [25, 26], measurements were acquired in the logarithmic mode in Fl-3 and calculated by setting gates over the first three decades to detect apoptotic cells. Dead cells are positive for propidium iodide and stained red, living cells remain unstained. In the logarithmic histogram the positions of unstained living cells in a are in the first 2 decades the 3th decade contains cells with membrane damage, dead cells are placed in the 4th decade.

Results

Time-Course of Cell Growth and comet formation in DU 145 prostate cancer and TP 366 glioblastoma cells provoked by TMZ and TMZ-BioShuttle dilution series

Two different cell lines originating from different tumor entities like the metastatic human prostate epithelium adenocarcinoma, herein referred as DU 145 (Figures 1-2) and TP 366 cells derived from human glioblastoma (Figures 3-4) were used to investigate the pharmacological effect of TMZ and TMZ-BioShuttle.

To learn more about the DNA damage and cell death in the two different cell lines after treatment with TMZ as well as with TMZ-BioShuttle using the identical dilution series, we carried out comet assays in parallel probes (right columns of the figure 1 and 2). Basically the untreated cultures of DU 145 prostate cancer cells and TP 366 cells did not exhibit fragmented DNA.

DU 145 Prostate cancer cells

In order to determine the sensitivity of these cells we used a dilution series in a range from 50 to 6.25 µM of TMZ and TMZ-BioShuttle respectively.

Two days after treatment with the TMZ final concentrations 6.25, 12.5 and 25 µM, the DU 145 cells seemed to be unfazed and no visual change in the phenotype could be observed under the light microscope. Counting the corresponding cell numbers offered a hardly detectable decrease of the cell number (from 1.15 to 1.05×10^6 cells) if anything compared to the untreated control with 1.12×10^6 cells. Only the probe treated with 25 µM TMZ revealed a decrease to 0.844×10^6 cells (Figure 1). The comet assay study indicated a higher sensitivity and exhibits fragmented DNA in the probes which were treated with 12.5, 25 and 50 µM TMZ. The samples treated with 50 µM TMZ displayed a decrease of the cell number to 0.628×10^6. Additionally in the cell culture medium an increasing number of dead, clumped DU 145 cells could be observed.

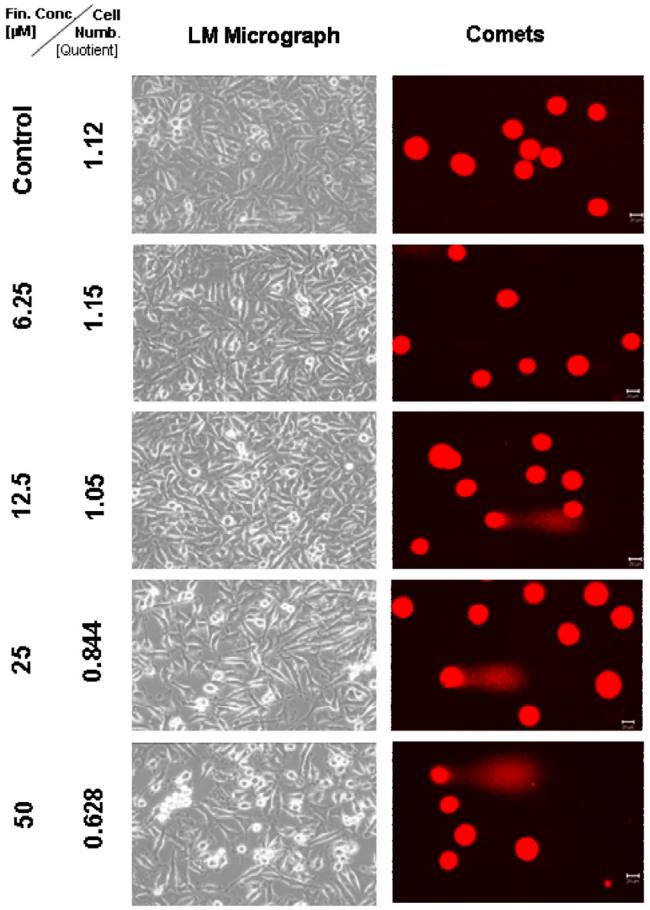

Figure 1 Microscopical monitoring of the human prostate cancer DU 145 cells 2 days after treatment with TMZ. In the comet column the scale bar represents 20 µm. The microscopic pictures were taken in phase-contrast, enlargement 200×.

TP 366 glioblastoma cells

Light microscopical studies showed a reduced cell population after treatment with 6.25 µM TMZ for 6 days which was increased further diminished under two fold application doses (12.5; 25 µM) from 6.2×10^5 cells (untreated control) to 5.3; 4.8, and 2.1×10^5 cells. In the TP 366 cells the TMZ probe treated with 50 µM, however, the cell population remained at the level of the 25 µM treated cells (2.1×10^5 cells) and may reach a saturation level.

After 6 days treatment with 6.25 µM TMZ (figure 1 and 2) the TP 366 cells showed differently sized and fragmented dead cells, sporadic comet structures and shrunken nuclei. In relation to the increased application doses an increase of fractionated DNA and shrunk nuclei could be observed. The TP 366 probe treated with 50 µM TMZ exhibited sporadic comets and almost condensed nuclei. The probes treated with TMZ-BioShuttle displayed a deviant behavior. The 6.25 µM TMZ-BioShuttle treated cells offer no DNA fragmentation, but their nuclei seemed to be partly swollen and diminished (figure 2). The latter fraction was increasing in accordance to the increased application doses. In addition the total cell count of the TMZ treated samples was lower, compared to the cell number in the control and cells treated with TMZ-BioShuttle.

The comet assay study detected no DNA fragmentation in the untreated control TP 366 cells until 144 hours. After application of TMZ-BioShuttle (6.25 µM) and more, much more DNA-fragments could be observed (figure 4). Indeed the use of higher application doses enhanced DNA fragmentations and the ratios of shrunk nuclei of TP 366 (figure 4 right column).

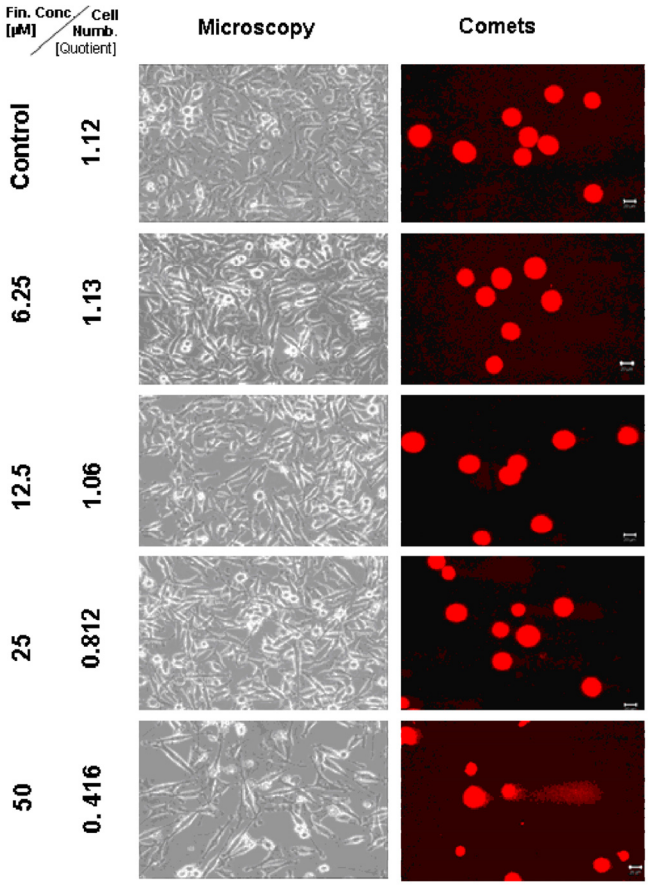

Figure 2 Microscopical monitoring of the human prostate cancer DU 145 cells 2 days after treatment with TMZ-BioShuttle. In the comet column, the scale bars in the maps represent 20 µm. The microscopic pictures were taken in phase-contrast, enlargement 200×.

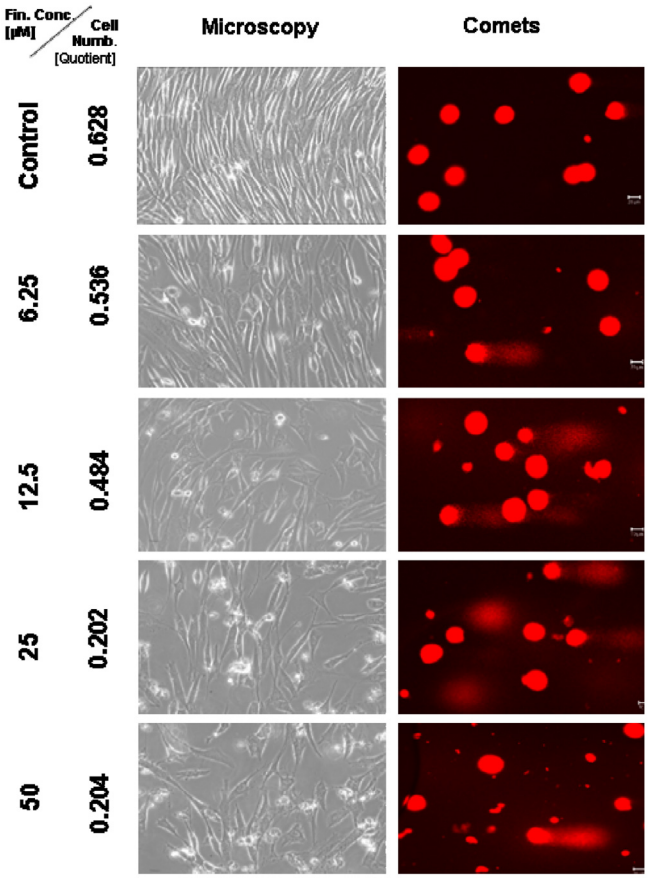

Figure 3 Microscopic and comet assay studies of untreated TP 366 cells and treated with various concentrations of TMZ; the scale bar represents 20µm.

Cell Cycle Studies

Here we present measurements of the cell activities like the cell cycle analysis using the flow cytometric method and a calculation of the percentage of cells in different phases of the cell cycle. These data were obtained after treatment with TMZ and the TMZ-BioShuttle in depency on the application dose. We determined the cell cycle behaviour of TP 366 glioma cells and DU 145 prostate cancer cells. To investigate the influence of TMZ with and without BioShuttle transporter we performed a dose-response analysis of the cell cycle shown in Figures 5 and 6.

TP 366 glioblastoma cells treated by TMZ and TMZ-BioShuttle dilution series

Figure 5 exhibits the cell cycle distribution of TP 366 cells 6 days after treatment with increasing concentrations of TMZ and TMZ-BioShuttle is shown in figure 5. The cell cycle distribution is signed as G1 phase, S phase and the G2/M phase. These cells show a diploid cycle (red coloured). The plot of the untreated control is demonstrated (figure 2, line 1) and exhibits a G1 cell fraction of 86.4 % and a G2 cell fraction 5.7 %. Looking the TMZ treated cells the contingent of cells in the S phase amounts to 7.8 %. In comparison to the S phase fraction of untreated control the percentage of S phase cells treated with 6.25 µM TMZ is increased to 11.1 %. The doubling of the TMZ dose to 12.5 µM results in a slightly decrease of the S phase fraction to 9.4 %. The further increase of the TMZ concentration to 25 µM and 50 µM has barely influenced the amount of the cells in the S phase with 9.1 % and 9.8 % respectively. Regarding the G2 phase we observed a dose dependent linear increase of the cell ratio. A concentration of 6.25 µM depicted an increase of cells from 5.7 % (control) to 10.2 %. The TMZ dose of 12.5 µM results in a scarcely increase to 10.7 %, but the doubling of the TMZ concentration to 25 µM and further to 50 µM resulted in an intense increase of the cell fraction in the G2/M phase with 15.9 % and 21.3 % respectively. The analysis of the dose dependent effect on the G1 phase exhibited the following trend: the starting dose rate was 6.25 µM TMZ, doubling of the doses to 25 and to 50 µM showed a reciprocal proportionality to the percentage of G1 cells, 74.8% and 68.8% (figure 2, right column).

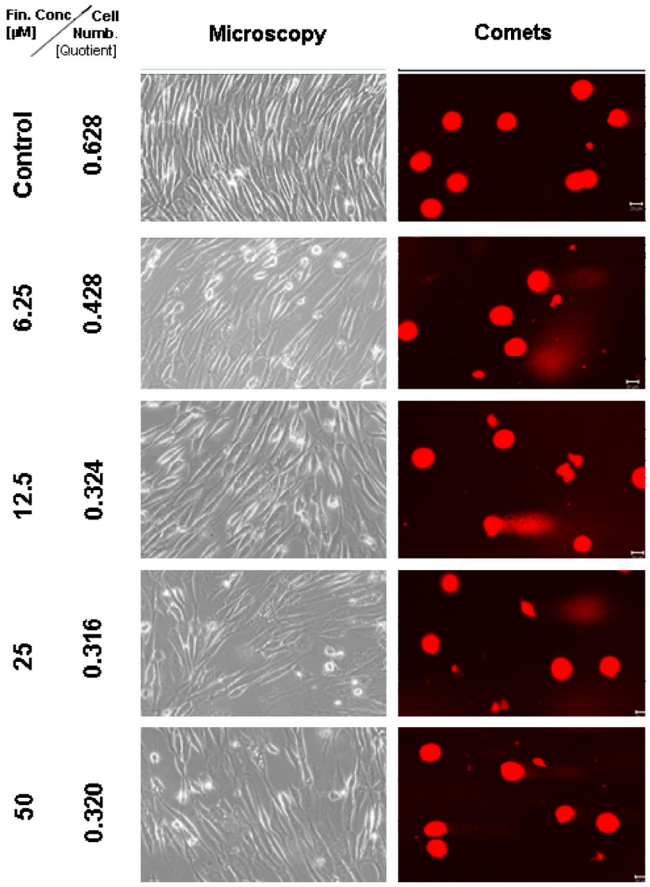

Figure 4 Microscopic and comet assay of untreated TP 366 glioblastoma cells, and 6 days after treatment with TMZ-BioShuttle; the scale bar represents 20µm. Microscopic magnification is 200-fold in the phase contrast microscope.

The TMZ-BioShuttle treated TP 366 cells presented a cell cycle behaviour strongly differing from the untreated control and from the TMZ treated cells.

The probe treated with 6.25 µM evidenced a reduced cell fraction in G1 phase of 70.6% already. The TP366 cells treated with doses 12.5 and 25 µM indicate G1 ratios of 57.9 and 37.6% respectively. Especially the data of the G2/M phase are demonstrative. From 6.25 µM up to 25 µM we observed an increase of the ratio of cells in G2/M from 19.1 %, via 28.6 % to 37.6 %. In comparison with the corresponding TMZ data, we found a continuous G2/M enhancement with the factor 2 starting at 6.25 µM! to 25 µM and a factor 3 in the probes treated with 12.5 µM.

Due to the high amount of dead cells the estimation of the cell cycle distribution in TP 366 cells treated with 50 µM TMZ-BioShuttle was difficult to perform and to analyse. It shows an increase of the cell fraction in the G1 phase to 68.8% which is identical to the corresponding probe treated with TMZ. Consistently increased amounts of the S phase cells could be detected compared to both the S phase in the control and the corresponding probes treated with TMZ. The trend of G2/M phase cells turned to the opposite direction. In the S phase not definitive trend arose from the applied dose.

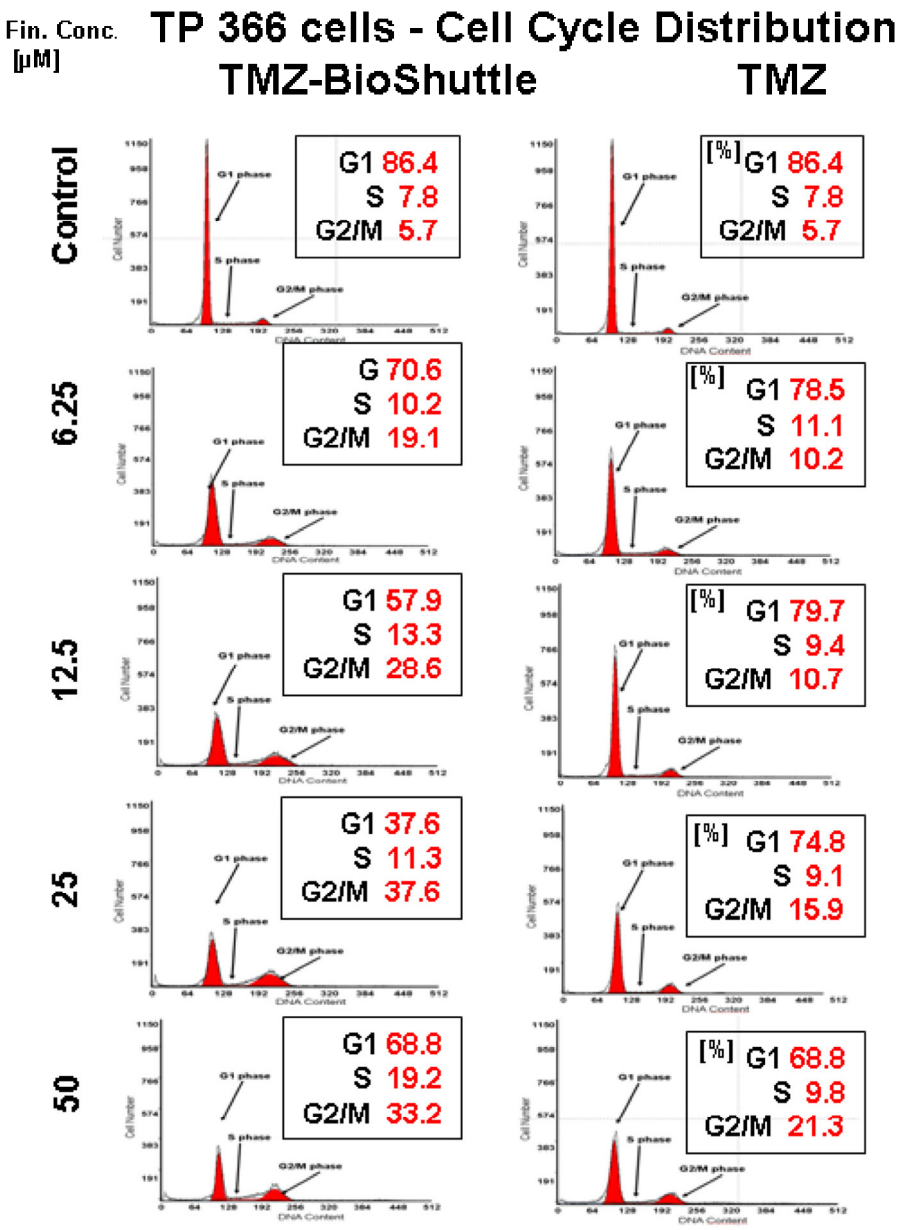

Figure 5 The cell cycle distribution in TP 366 glioblastoma cells dependent on the applied concentration of TMZ (right column) and TMZ-BioShuttle (left column) 6 days after treatment. The axes of coordinates represent the cell number; the abscissae represent the corresponding DNA content. The left peak depicts the amount of cells in the G1 phase; the area of the right peak describes the ratio of cells in the G2/M phase. The area between both peaks displays the amount of the cell fraction residing in the S phase. The insert describes the percentage of cells in the phases of the cell cycle.

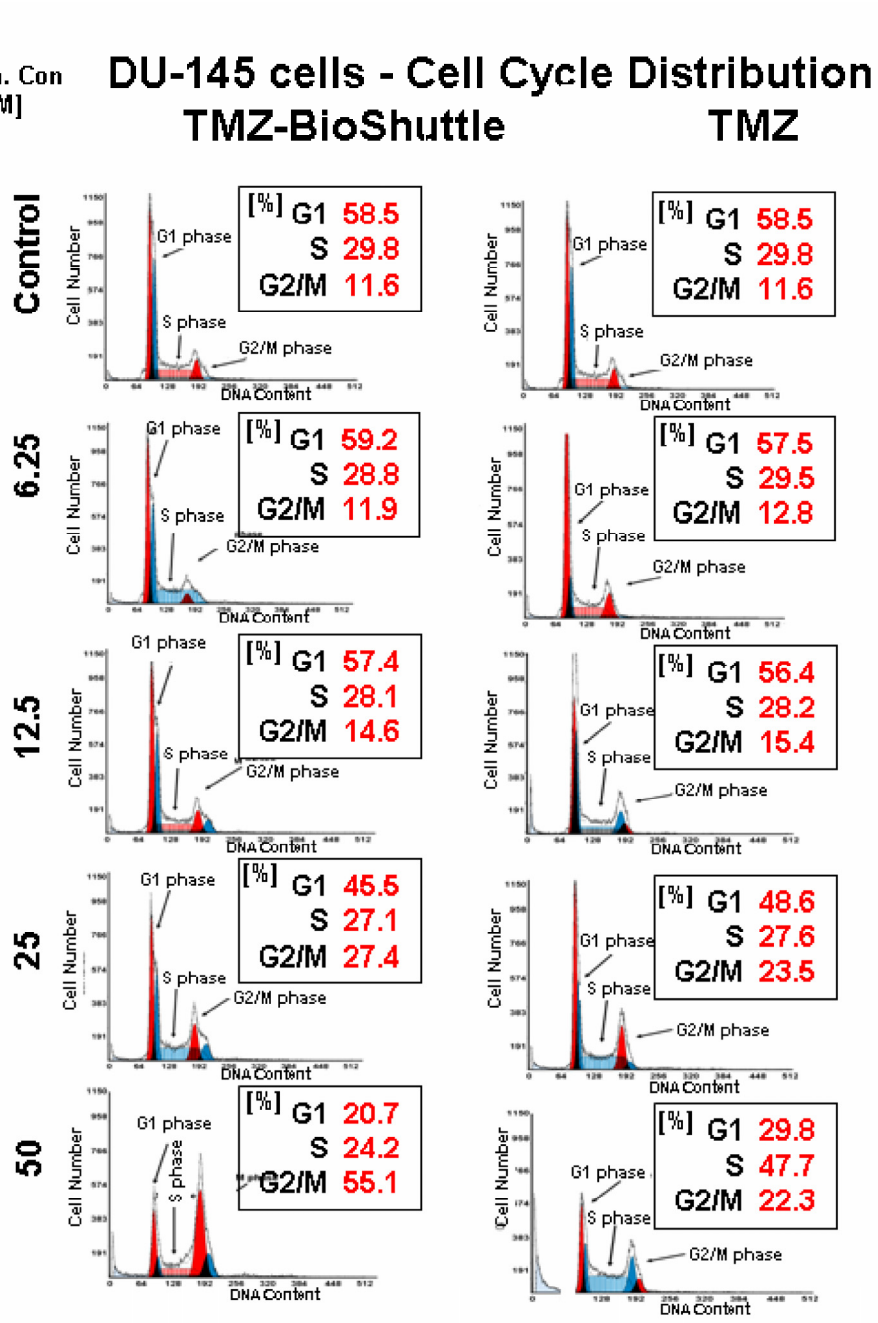

Figure 6 The cell cycle ratio of DU 145 prostate cancer cells dependent on the applied concentration of TMZ (right column) and TMZ-BioShuttle (left column) 2 days after treatment. The axes of coordinates represent the cell number; the abscissae represent the corresponding DNA content. The left peak depicts the amount of cells in the G1 phase; the area of the right peak describes the ratio of cells in the G2/M phase. The area between both peaks displays the amount of the cell fraction residing in the S phase.

Cell cycle behaviour of DU 145 cells after treatment with TMZ and TMZ-BioShuttle dilution series

At a first glance the histograms reveal a lower sensitivity of DU 145 prostate cells against TMZ treatment compared to the results of TP 366 cells. The untreated DU 145 control exhibits a cell cycle distribution as follows: G1 – 58.5%; S phase – 29.8% and G2/M phase 11.6%. The ratio of TMZ treated cells in the G2/M phase amounts to 12.8%; 15.4% and 23.5% and is constantly increasing in correlation to the application doses of 6.25; 12.5 and 25 µM.

The percentage of the S phase cells after treatment with the above described concentrations were almost constant 29.5% and close to the control. The cells in the G1 fractions treated with increasing concentrations up to 25 µM of TMZ presented a moderate but uniform, continuous decrease from 58.5% (control), via 57.5%, 56.4%, to 48.6 % and then a strong decline to 29.8%. The DU 145 probe treated with 50 µM TMZ showed 22.3% G2/M phase cells and a dramatic increase of the S phase cell fraction to 47.7%.

The DU 145 cells treated with the TMZ-BioShuttle under identical conditions offered a cell cycle behaviour which strongly differs from the TMZ probes. The percentage of cell fractions in G1 phase seemed to be nearly constant 58.5% comparing the untreated control versus the treated cells with concentrations 6.25µM 59.2 %and 12.5 µM 57.4%. The concentrations of 25 and 50 µM gave rise to a marked decrease of the percentage of cells from 45.5% to 20.7% in G1 which corresponds to one-third of the related TMZ treated probe!

The relative amounts of S phase cells in the concentration series with increasing TMZ-BioShuttle doses of 6.25, 12.5, 25, and 50 µM offered a reciprocal proportionality and showed a small but continuous decrease of cell number from 29.8% (control), via 28.8%, 28.1%, 27.1%, to 24.2% respectively. It is important to note that the latter result showed a strong reduction comparing 47.7% (TMZ) to 24.2% (TMZ-BioShuttle) which equates a degression of 50%. The concentration series with increasing amounts of TMZ-BioShuttle indicated a direct concentration dependence and displayed a moderate increase of the cell number of DU 145 cells in the G2/M fraction from 11.6% (control) to 11.9% in the 6.25 µM probe via 12.5, 25 to 50 µM. A strong rise of the S phase cells from 14.6% via 27.4% to 55.1% was shown. Doubling the applied dose increased cell number in the G2/M phase mote than 100%! Additionally, the direct comparison of the probe treated with 50 µM TMZ-BioShuttle with the corresponding TMZ probe of DU 145 cells showed a dramatic increase in the percentage of cells in the G2/M phase (from 22.3% to 55.1%), revealing a G2/M block.

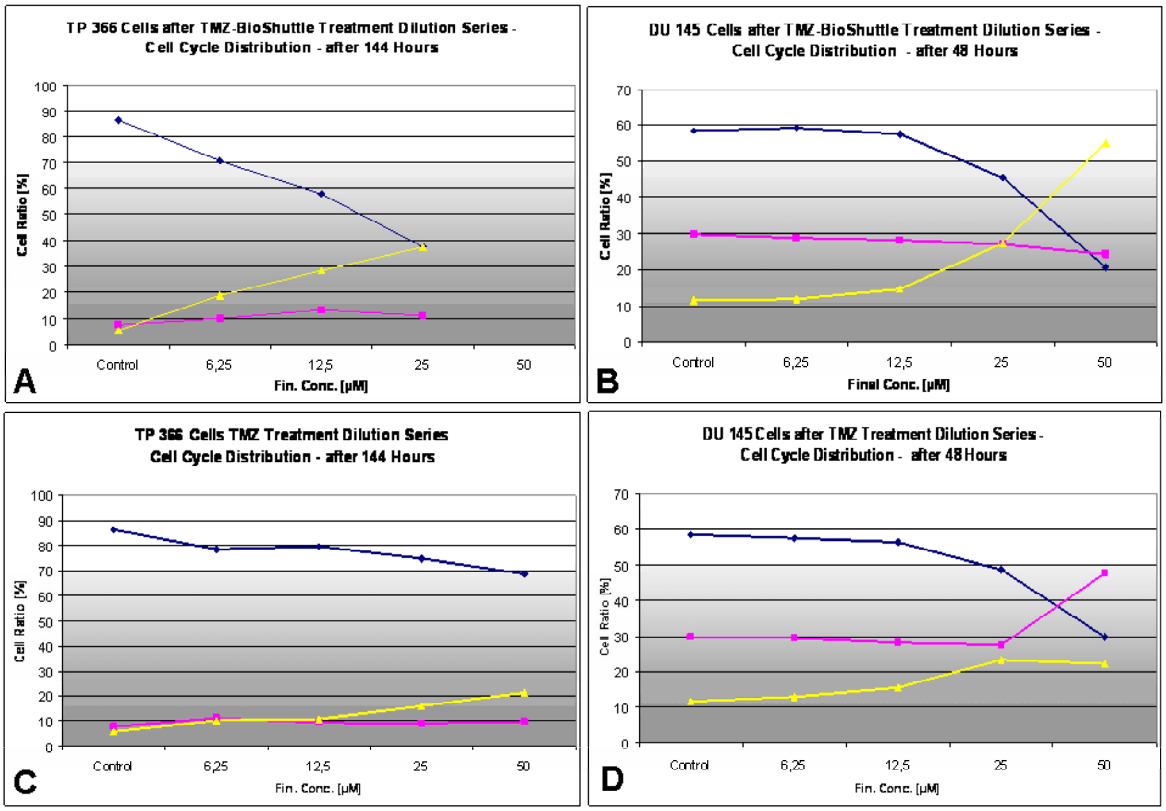

Figure 7 The dose dependent effects of TMZ (C/D) as well as TMZ-BioShuttle (A/B) in the cell cycle behaviour of TP366 glioma (A/C) and DU 145 prostate cancer (B/D) cells. ♦ G1phase; ■ S phase; ▲ G2/M phase

Discussion

The number of old-fashioned cytotoxic drugs, whose effectiveness is well understood, is multi-faced. However, if highly effective substances do not reach their target site after application, what is their benefit? Therefore questions about the bioavailability remain to be answered, whereby the concentration in the blood-stream is not meant here, but rather the concentration directly at the site of pharmacological action, like the genomic DNA in tumor cell nuclei.

A substantial progress in the drug development will be achieved by improvement of the delivery and subcellular targeting of the drug as yet unappreciated and meaningless.

The BioShuttle delivery and targeting platform, facilitating the transport of DNA derivatives into living cells was described [27, 28] as well as transport of diagnostics into the cytoplasm and nuclei of tumor tissues [29, 30]. There is no doubt that constructs like the TMZ-BioShuttle, as an example, could play a helpful role in the treatment of cancer. The design of such shuttles needs to incorporate features that reduce undesired adverse reactions but maintains the efficacy.

We selected the highly efficient chemotherapeutic TMZ as a qualified candidate, since encouraging results in treatment of in brain tumors [31] remain unendorsed in the treatment of hormone-refractory prostate cancer (HRPC) [32].

Parallel sets of experiments with TP 366 glioma cells and DU 145 prostate cancer cells were carried out and confirmed a lesser sensitivity of DU 145 prostate cancer cells against TMZ treatment. Whereas the TP 366 cells showed an increased DNA damage after TMZ treatment up to a final concentration of 6.25 µM, the DU 145 cells exhibited very few DNA damage measured by comet assay. The increase of the application dose however did not induce an increased number of comets (figure 1). This phenomenon was already documented in studies with ceramide-induced cell death [33].

In DU 145 cells we compared the dose-dependent application of TMZ and TMZ-BioShuttle of seeded versus harvested cells after 48 hours. In comparison to the control (1.12) a linear inverse proportionality (1.15; 1.05; 0.844; and 0.628) to the dilution series of 6.25; 12.5; 25; and 50 µM TMZ was demonstrated.

These data permit to assume a minimum of TMZ application dose between 25 and 12.5 µM. Dilution series with 50 µM to 6.25 µM of TMZ-BioShuttle showed an increase of shrunk nuclei (figures 2 and 4). The TMZ-BioShuttle revealed the identical subthreshold in DU 145 cells but the quotient 0.414 at 50 µM suggests a higher pharmacological potential.

The results achieved with both cell lines (TP 366 and DU 145) treated with the TMZ-BioShuttle differ in the expected augmentation of DNA comets: All cells were visibly swollen, but we could not detect an increased number of comets. This suggests a decondensation of chromatin in the nuclei. This happens when chromosomes are exposed to DNA replication inhibition caused by failure to constitute compact chromatin areas during mitosis [34]. It could be explained with the involvement of the transcription of genes expressing histone regulating proteins responsible for formation of the chromatin structure and for the compact package of DNA [35].

We investigated the cell cycle of TP366 after treatment of the glioblastoma cells with TMZ. It interfered with the cell cycle and exhibited a decreased number of cells in the S phase fraction as shown 144 hours after TMZ-application when a contingent of the S phase cells of 8% was detectable.

The phenomenon of a reduced S phase (8% versus control 11%) in the TMZ treated TP 366 cells is not contradictory to the common effects of alkylating agents which cause a retardation of the rate of cell division [36]. A possible explanation for the strongly decreased S phase cell number in the TMZ-BioShuttle treated probes would be the existence of a S phase cell cycle arrest as documented in a bimodal TMZ/ interferon-β (IFN-β) study [37]. Our flow cytometry experiments also displayed a strong cell cycle arrest in the S phase [38]. An interesting criterion for a prolonged late S/G2 phase suggests the implication of the histone acetyltransferase 1 (HAT1) which participates in recovering block-mediated DNA damages [39].

The fact that the glioblastoma cells arrest in the G2/M phase after TMZ-treatment was documented by Hirose et al. [40] and could be confirmed with the TP 366 cells. Moreover the treatment with TMZ-BioShuttle resulted in a clearly increased G2/M phase of 72%. It seems to be attributed to interactions of TMZ and TMZ-BioShuttle with the mitogen-activated protein (MAP) kinase p38α, which is activated by the mismatch repair system (MMR) and is responsible for the TMZ-induced G2/M block [40].

After cell exposure to the TMZ-BioShuttle for 144 hours, the observed strong increase of the G2 phase cells of TP 366 cells possibly originate from the already documented inhibition of the RNA and protein syntheses, which are necessary for the successful completion of G2 and the initiation of mitosis. These G2-arrested cells were found to be deficient in certain proteins that may be specific for the G2-mitotic transi-

tion [41]. The obstruction of the cell cycle process is caused by the stop of this transition and results in the decrease of the G1 phase cell fraction (26%) of the TMZ-BioShuttle treated TP 366 cells which appear to be consequence of their disability passing in the mitotic process.

A sensitivity of DU 145 and TP 366 cells against TMZ and a dramatically increased sensibility against TMZ-BioShuttle is shown in figure 4. The present data document a different cellular contumaciousness to TMZ treatment. A real effectiveness of the pure TMZ in DU 145 cells could not be observed, whereas in contrast clear cell killing effects, caused by TMZ-BioShuttle, were detected.

It is important to note that the TMZ-BioShuttle treatment of DU 145 and the TP 366 cells redounds to cell killing effects as shown in figure 4.

As a general rule the different sensitivity of tumor cells against chemotherapeutics is dependent on multiple mechanisms like multiple drug resistance systems. The relative low sensitivity of DU 145 prostate cancer cells after treatment with TMZ is evident, and the disappointing results of TMZ trials of prostate cancer can be explained by the increased O^6-methylguanine-DNA methyltransferase (MGMT) repair activity. DU 145 cells show an increased MGMT activity [42], associated with the decrease of the pharmacologic effect after alkylating with TMZ alone. The increased MGMT expression and activity correlates with the malignant phenotype [43]. We regard the potential utility of this epigenetic alteration as an appropriate biomarker for prostate cancer [44] and an important prognostic feature for the clinical outcome in glioblastoma [45]. The fact that die blood brain barrier (BBB) no presents an hurdle for TMZ could explain the higher pharmacological effects of TMZ in glioma cells. It is important in so far that the delivery and the targeting of active substances play a decisive role and must be further scrutinized. The TMZ-BioShuttle could be an appropriate candidate.

The physico-chemical properties of TMZ which have an impact on its bioavailability limit its pharmacological effectiveness. Despite the benefit of the concomitant treatment with radiotherapy plus TMZ, hematologic toxic effects in patients treated with TMZ are documented in multicenter studies by Stupp [46]. A TMZ-derivatization with targeting transporters molecules and subcellular address components holds tremendous potential to optimize treatment of diseases. Enhanced cellular delivery and active transport of TMZ into the cell nuclei as site of pharmacological action permit to expect lower application doses with concomitantly decreased limiting side-effects.

Our shuttle, designed for facilitating the rapid transport across cellular membranes, improved their own delivery and their own targeting under perpetuation of the pharmacological activity in cells and tissues while protecting cells in the bloodstream by omission of undesired side-effects like:

Strong suppression of the peripheral lymphocytes result in discontinuation of therapy and problems associated with systemic drug administrations, which are:

- even biodistribution of pharmaceuticals throughout the body;
- the lack of drug specific affinity toward a pathological site;
- the necessity of a large total dose of a drug to achieve high local concentration;
- non-specific toxicity and strong adverse side-effects due to high drug doses [47, 48].

The application of the TMZ-BioShuttle could minimize the handicap of TMZ on the therapy of patients with brain tumors but the establishment of the TMZ-BioShuttle necessitates new ways for the synthesis. Conditions which hampered the above postulated criteria like rapid and whole concurrent chemical reactions in aqueous solution at room temperature for a proper chemical ligation of functional peptides could be circumvented using the 'inverse-electron-demand' of the Diels Alder Reaction.

Thus, TMZ-BioShuttle has been reformulated to decrease the toxic features in normal cells but retain the pharmacologic behavior in target cells; this was achieved as follows: coupling the amide group of the TMZ with a tetrazine which acts as dien-component and connects the NLS module with the tridecadien (TCT) component operating as dienophil.

The presented publication shows that a proper chemistry contributes to the optimization of the pharmacological properties of the already efficient pharmaceutics like TMZ.

The novel properties of the TMZ-BioShuttle could give reason to the extension to tumor types like prostate cancer, especially in hormone refractory situations.

Abbreviations

DAR: Diels-Alder-Reaction, GBM: Glioblastoma Multiforme, HAT1: Histone Acetyltransferase 1, IFN-β: Interferon-β, MGMT: Methylguanine-DNA-Methyltransferase, NLS: Nuclear Localization Sequence, TCT: Tetracyclo-[5.4.$2^{1,7}$.$O^{2,6}$.$O^{8,11}$] 3,5-dioxo-4-aza-9,12-tridecadien, TMZ: Temozolomide.

Acknowledgements

The work in this article was done in close collaboration with Peter Lorenz and Heinz Fleischhacker of our group. We cordially thank Dr. Christian Kliem and Dr. Jochen vom Brocke for critically reading the manuscript and stimulating discussions.

Conflict of Interest

We declare no conflicts of interest.

References

1. Lambert T, Recht M, Valentino LA, et al. Reformulated BeneFix: efficacy and safety in previously treated patients with moderately severe to severe haemophilia B. Haemophilia. 2007; 13: 233-43.
2. Johnson JL, Yalkowsky SH. Reformulation of a new vancomycin analog: an example of the importance of buffer species and strength. AAPS PharmSciTech. 2006; 7: E5.
3. O'Riordan TG. Optimizing delivery of inhaled corticosteroids: matching drugs with devices. J Aerosol Med. 2002; 15: 245-50.
4. Roy V, Perez EA. New therapies in the treatment of breast cancer. Semin Oncol. 2006; 33: S3-S8.
5. Marchesi F, Turriziani M, Tortorelli G, et al. Triazene compounds: mechanism of action and related DNA repair systems. Pharmacol Res. 2007; 56: 275-87.
6. Danson SJ, Middleton MR. Temozolomide: a novel oral alkylating agent. Expert Rev Anticancer Ther. 2001; 1: 13-9.
7. Shinoura N, Yamada R, Tabei Y, et al. [Temozolomide-temodal.]. Gan To Kagaku Ryoho. 2008; 35: 543-7.
8. Mutter N, Stupp R. Temozolomide: a milestone in neuro-oncology and beyond? Expert Rev Anticancer Ther. 2006; 6: 1187-204.
9. Denny BJ, Wheelhouse RT, Stevens MF, et al. NMR and molecular modeling investigation of the mechanism of activation of the antitumor drug temozolomide and its interaction with DNA. Biochemistry. 1994; 33: 9045-51.
10. Cai Y, Wu MH, Xu-Welliver M, et al. Effect of O6-benzylguanine on alkylating agent-induced toxicity and mutagenicity. In Chinese hamster ovary cells expressing wild-type and mutant O6-alkylguanine-DNA alkyltransferases. Cancer Res. 2000; 60: 5464-9.
11. Hirose Y, Kreklau EL, Erickson LC, et al. Delayed repletion of O6-methylguanine-DNA methyltransferase resulting in failure to protect the human glioblastoma cell line SF767 from temozolomide-induced cytotoxicity. J Neurosurg. 2003; 98: 591-8.
12. Riccardi A, Mazzarella G, Cefalo G, et al. Pharmacokinetics of temozolomide given three times a day in pediatric and adult patients. Cancer Chemother Pharmacol. 2003; 52: 459-64.
13. Kolb HC, Sharpless KB. The growing impact of click chemistry on drug discovery. Drug Discov Today. 2003; 8: 1128-37.
14. Kolb HC, Finn MG, Sharpless KB. Click Chemistry: Diverse Chemical Function from a Few Good Reactions. Angew Chem Int Ed Engl. 2001; 40: 2004-21.
15. Kohn M, Breinbauer R. The Staudinger ligation-a gift to chemical biology. Angew Chem Int Ed Engl. 2004; 43: 3106-16.
16. Chandra RA, Douglas ES, Mathies RA, et al. Programmable cell adhesion encoded by DNA hybridization. Angew Chem Int Ed Engl. 2006; 45: 896-901.
17. Rostovtsev VV, Green LG, Fokin VV, et al. A stepwise huisgen cycloaddition process: copper(I)-catalyzed regioselective "ligation" of azides and terminal alkynes. Angew Chem Int Ed Engl. 2002; 41: 2596-9.
18. Bachmann WE, Deno NC. The Diels-Alder Reaction of 1-Vinylnaphthalene with a,@- and a,p,y,G- Unsaturated Acids and Derivatives. J Americ Chem Soc. 1949; 71: 362-3.
19. Reppe W, Schlichting O, Klager K, et al. Cyclisierende Polymerisation von Acetylen I. Justus Liebigs Annalen der Chemie. 1948; 560: 1-92.
20. Merriefield RB. Solid Phase Peptide Synthesis. I The Synthesis of a Tetrapeptide. J Americ Chem Soc. 1963; 85: 2149-54.
21. Ahn JY, Hu Y, Kroll TG, et al. PIKE-A is amplified in human cancers and prevents apoptosis by up-regulating Akt. Proc Natl Acad Sci U S A. 2004; 101: 6993-8.
22. Stone KR, Mickey DD, Wunderli H, et al. Isolation of a human prostate carcinoma cell line (DU 145). Int J Cancer. 1978; 21: 274-81.
23. Ehemann V, Sykora J, Vera-Delgado J, et al. Flow cytometric detection of spontaneous apoptosis in human breast cancer using the TUNEL-technique. Cancer Lett. 2003; 194: 125-31.
24. Nicoletti I, Migliorati G, Pagliacci MC, et al. A rapid and simple method for measuring thymocyte apoptosis by propidium iodide staining and flow cytometry. J Immunol Methods. 1991; 139: 271-9.
25. Singer S, Ehemann V, Brauckhoff A, et al. Protumorigenic overexpression of stathmin/Op18 by gain-of-function mutation in p53 in human hepatocarcinogenesis. Hepatology. 2007;46(3):759-68.
26. Tschaharganeh D, Ehemann V, Nussbaum T, et al. Non-specific Effects of siRNAs on Tumor Cells with Implications on Therapeutic Applicability Using RNA Interference. Pathol Oncol Res. 2007; 13: 84-90.
27. Braun K, Peschke P, Pipkorn R, et al. A biological transporter for the delivery of peptide nucleic acids (PNAs) to the nuclear compartment of living cells. J Mol Biol. 2002; 318: 237-43.
28. Braun K, von BL, Pipkorn R, et al. BioShuttle-mediated plasmid transfer. Int J Med Sci. 2007; 4: 267-77.
29. Heckl S, Debus J, Jenne J, et al. CNN-Gd(3+) Enables Cell Nucleus Molecular Imaging of Prostate Cancer Cells: The Last 600 nm. Cancer Res. 2002; 62: 7018-24.
30. Heckl S, Pipkorn R, Waldeck W, et al. Intracellular Visualization of Prostate Cancer Using Magnetic Resonance Imaging. Cancer Res. 2003; 63: 4766-72.
31. Newlands ES, Blackledge GR, Slack JA, et al. Phase I trial of temozolomide (CCRG 81045: M&B 39831: NSC 362856). Br J Cancer. 1992; 65: 287-91.
32. van Brussel JP, Busstra MB, Lang MS, et al. A phase II study of temozolomide in hormone-refractory prostate cancer. Cancer Chemother Pharmacol. 2000; 45: 509-12.
33. Monti B, Zanghellini P, Contestabile A. Characterization of ceramide-induced apoptotic death in cerebellar granule cells in culture. Neurochem Int. 2001; 39: 11-8.
34. Lukusa T, Fryns JP. Human chromosome fragility. Biochim Biophys Acta. 2008; 1779: 3-16.
35. Kristeleit R, Stimson L, Workman P, et al. Histone modification enzymes: novel targets for cancer drugs. Expert Opin Emerg Drugs. 2004; 9: 135-54.
36. Bignold LP. Alkylating agents and DNA polymerases. Anticancer Res. 2006; 26: 1327-36.
37. Park JA, Joe YA, Kim TG, et al. Potentiation of antiglioma effect with combined temozolomide and interferon-beta. Oncol Rep. 2006; 16: 1253-60.
38. Thomas HC, Lame MW, Wilson DW, et al. Cell cycle alterations associated with covalent binding of monocrotaline pyrrole to pulmonary artery endothelial cell DNA. Toxicol Appl Pharmacol. 1996; 141: 319-29.
39. Barman HK, Takami Y, Ono T, et al. Histone acetyltransferase 1 is dispensable for replication-coupled chromatin assembly but contributes to recover DNA damages created following replica-

tion blockage in vertebrate cells. Biochem Biophys Res Commun. 2006; 345: 1547-57.
40. Hirose Y, Katayama M, Stokoe D, et al. The p38 mitogen-activated protein kinase pathway links the DNA mismatch repair system to the G2 checkpoint and to resistance to chemotherapeutic DNA-methylating agents. Mol Cell Biol. 2003; 23: 8306-15.
41. Rao PN. The molecular basis of drug-induced G2 arrest in mammalian cells. Mol Cell Biochem. 1980; 29: 47-57.
42. Xie CH, Naito A, Mizumachi T, et al. Mitochondrial regulation of cancer associated nuclear DNA methylation. Biochem Biophys Res Commun. 2007; 364: 656-61.
43. Patra SK, Patra A, Zhao H, et al. DNA methyltransferase and demethylase in human prostate cancer. Mol Carcinog. 2002; 33: 163-71.
44. Nakayama M, Gonzalgo ML, Yegnasubramanian S, et al. GSTP1 CpG island hypermethylation as a molecular biomarker for prostate cancer. J Cell Biochem. 2004; 91: 540-52.
45. Hegi ME, Liu L, Herman JG, et al. Correlation of O6-methylguanine methyltransferase (MGMT) promoter methylation with clinical outcomes in glioblastoma and clinical strategies to modulate MGMT activity. J Clin Oncol. 2008; 26: 4189-99.
46. Stupp R, Mason WP, van den Bent MJ, et al. Radiotherapy plus concomitant and adjuvant temozolomide for glioblastoma. N Engl J Med. 2005; 352: 987-96.
47. Torchilin VP. Drug targeting. Eur J Pharm Sci. 2000; 11 (Suppl 2): S81-S91.
48. Braun K, Pipkorn R, Waldeck W. Development and Characterization of Drug Delivery systems for Targeting Mammalian Cells and Tissues: A Review. Curr Med Chem. 2005; 12: 1841-58.